Spike-timing-dependent plasticity induction reveals dissociable supplementary– and premotor–motor pathways to automatic imitation

Spike-timing-dependent plasticity induction reveals dissociable supplementary– and premotor–motor pathways to automatic imitation

Sonia Turrini[a,1], Francesca Fiori[a,b,2], Naomi Bevacqua[a,c,2], Chiara Saracini[d], Boris Lucero[d], Matteo Candidi[c], and Alessio Avenanti[a,d,1]

Author affiliations: [a]Centro studi e ricerche in Neuroscienze Cognitive, Dipartimento di Psicologia "Renzo Canestrari", Campus di Cesena, Alma Mater Studiorum Università di Bologna, 47521 Cesena, Italy; [b]Neurophysiology and Neuroengineering of Human- Technology Interaction Research Unit, Università Campus Bio-Medico di Roma, 00128 Roma, Italy; [c]Dipartimento di Psicologia, Sapienza Università di Roma, 00185 Roma, Italy; and [d]Centro de Investigación en Neuropsicología y Neurociencias Cognitivas, Universidad Católica Del Maule, 3460000 Talca, Chile

Introduction

Humans tend to tune their behavior to that of other individuals (1, 2). The impulse to reproduce observed actions, even when irrelevant to the current task, is termed automatic imitation (2, 3) and can be captured in ecological situations (1, 4), as well as in experimental settings, using controlled behavioral methods such as the imitation inhibition task (5). This task assesses automatic imitation through a stimulus–response (S–R) compatibility paradigm rooted in an established tradition of psychology research (3, 5): participants perform an arbitrary visuomotor mapping task requiring to respond to a symbolic target cue by lifting a finger while seeing congruent or incongruent task-irrelevant finger movements on a screen. During congruent trials, the observed movement and the intended movement match, resulting in faster reaction times (RTs) and higher accuracy. Conversely, during incongruent trials, the observed movement differs from the intended movement, which creates a conflicting situation where the bottom–up automatic imitative tendency competes with the top–down goal-oriented behavior based on task rules, leading to lower speed and accuracy (3, 5, 6).

Automatic imitation is thought to rely on the bottom–up activation of motor nodes of the action observation network (AON) (2, 7–9), including the ventral premotor cortex (PMv), which in turn sends projections to the primary motor cortex (M1) (10). Thus, when seeing an action congruent with an intended act during congruent trials of the imitation inhibition task, AON bottom–up motor activations are thought to converge with the parallel activation of intentional S–R associations established for the purpose of the task, leading to faster RTs and higher accuracy (2, 3). Conversely, when seeing an action incongruent with the intended act during incongruent trials of the imitation inhibition task, a conflict arises between the bottom–up automatic imitative tendency and the top–down goal-oriented behavior based on task rules, leading to lower speed and accuracy (3, 5, 6). To solve this competition, additional neural resources are engaged (11–15). Among areas of the AON active under these conflict conditions, a potential role in controlling automatic imitation has been afforded to the supplementary motor area (SMA) (16). While the SMA is consistently found to be activated by both action observation and execution (8, 16, 17), invasive registration studies in monkeys

[1] correspondent authors: sonia.turrini2@unibo.it, alessio.avenanti@unibo.it

[2] equal contribution

and humans indicate that its neurons modulate their firing based on whether action execution is contextually adequate (18, 19) and can exhibit state-dependent properties switching from excitation during action execution to inhibition during action observation (20). Additionally, it has been proposed that the SMA exerts a "gating" function in the context of a domain-general role of motor control, controlling M1 activity to prevent inadequate overt motor behavior (16–18, 21).

Two competing hypotheses propose alternative roles of PMv in imitation. One suggests that ventral frontal regions such as the PMv and the adjacent inferior frontal gyrus primarily facilitate automatic imitation by mapping observed actions and transmitting excitatory signals to M1 (10, 22). Conversely, a competing hypothesis proposes that these regions may exert both inhibitory or facilitatory functions in controlling automatic imitation based on context and task features (23, 24; see also ref. 25). Therefore, the functional roles of PMv-to-M1 and SMA-to-M1 interactions in mediating automatic imitation and their possible dissociable contributions remain unclear due to the challenges of disentangling them using correlational imaging approaches.

To address this outstanding issue, we adopted a network-based brain stimulation approach. Rather than focusing on the role of isolated brain regions, we sought to establish the causal role and malleability of cortico-cortical projections from the AON to M1 in facilitating or controlling automatic imitation. Specifically, we tested whether driving Hebbian associative spike-timing-dependent plasticity (STDP) through cortico-cortical Paired Associative Stimulation (ccPAS) (25–30) of PMv-to-M1 or SMA-to-M1 connections affects performance in the imitation inhibition task.

Previous studies proved that the ccPAS protocol can strengthen or weaken directional cortico-cortical connectivity of the PMv-to-M1 (25, 28, 31, 32) and SMA-to-M1 neural pathways (33, 34), by modulating synaptic efficacy of premotor–motor projections. For example, administration of a $ccPAS_{PMv\rightarrow M1}$ protocol, involving repeated and sequential TMS activation of PMv followed by M1, increased the influence of the former over the latter, due to an increase in the synaptic efficacy of PMv-to-M1 cortico-cortical projections (25). Similar results were also obtained by applying ccPAS to the SMA-to-M1 circuit (33). Building on these advancements, the present study sought to test the competing theories about PMv and SMA involvement in the tendency to imitate others' actions. Eighty healthy participants were divided into four groups according to the administered ccPAS protocol (*SI Appendix*, Table S1). Tasks were performed before (Pre), immediately after (T0), and 30 min after (T30) ccPAS (Fig. 1*A*). Two protocols aimed at strengthening PMv-to-M1 ($ccPAS_{PMv\rightarrow M1}$ group) or SMA-to-M1 ($ccPAS_{SMA\rightarrow M1}$ group) directional connectivity. A $ccPAS_{M1\rightarrow PMv}$ group controlled for the protocol's directionality (25), and a sham ccPAS served as a control for unspecific effects ($ccPAS_{Sham}$ group).

Participants completed two tasks before and after the ccPAS intervention. The two tasks were selected to tap into automatic and voluntary imitation. To assess automatic imitation, we asked participants to perform an established imitation inhibition task that uses numbers as symbolic cues dictating task rules, and finger movements as task-irrelevant cues—i.e., the Number Task (5, 35) (Fig. 1*C*). To control for functional specificity, participants also performed a voluntary imitation task (Finger Task), where they were required to imitate the observed finger movements and ignore symbolic cues (i.e., numbers).

According to an established line of research, interference in the Number Task is due to competition between short-term (weaker) number-to-action associations established for the purpose of the task and long-term (stronger) finger-to-action associations (2, 3). In contrast, facilitatory effects are based on the convergence of goal-oriented (i.e., following the task rules) and automatic behavior (2, 3). We hypothesized that enhancing PMv-to-M1 connectivity (i.e., $ccPAS_{PMv\rightarrow M1}$) would enhance the propensity to automatically imitate task-irrelevant observed actions, clarifying the function of the PMv-M1 pathway within the AON, and that strengthening SMA-to-M1 connectivity ($ccPAS_{SMA\rightarrow M1}$) would reduce automatic imitation, providing causal evidence for SMA's gating function of imitation. Based on previous studies showing no net effect of premotor-M1 ccPAS on simple visuomotor tasks (26, 31, 34), we expected that ccPAS would exert little or no effect on trials that imply no competition between task-relevant and irrelevant stimuli (i.e., in neutral trials of both the Number and Finger tasks; see Fig. 1). Conversely, we expected that manipulation of PMv-to-M1 and SMA-to-M1 connectivity via STDP would affect automatic imitation, particularly the interference effect measured during incongruent trials that are associated with increased task demands (11–15).

To assess the build-up of associative plasticity in the targeted networks, we continuously monitored motor excitability via motor-evoked potentials (MEPs) during the ccPAS administration and expected their gradual increase during $ccPAS_{PMv\rightarrow M1}$ and $ccPAS_{SMA\rightarrow M1}$, underpinning the establishment of long- term potentiation (LTP) like effects (25, 26, 33, 36).

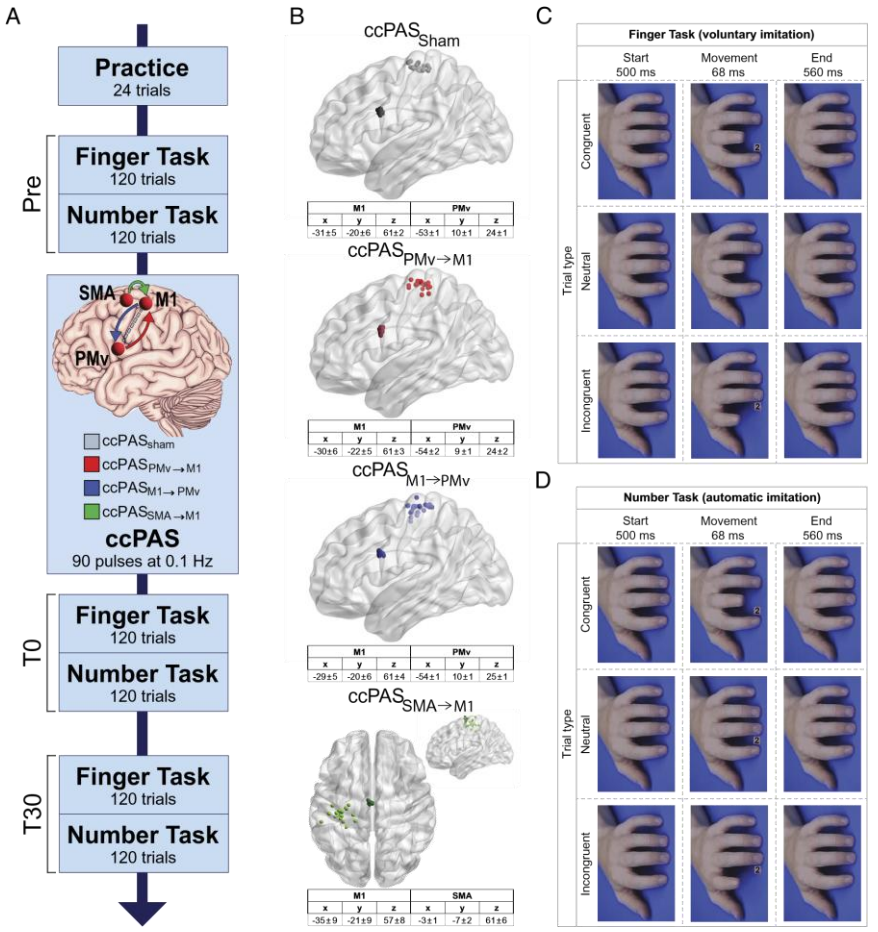

Fig. 1. (*A*) General experimental procedure. (*B*) Individual targeted brain sites reconstructed on a standard template using BrainNet after conversion to MNI space using Brett's algorithm. (*C*) Schematic depiction of the Finger Task with finger movements as the relevant dimension, tapping into overt imitation, and the numbers as the task-irrelevant feature; (*D*) schematic depiction of the Number Task with symbolic cues (numbers), as the relevant dimension and the finger movements as the task-irrelevant feature, tapping into automatic imitation. Hand images were displayed in vertical orientation to avoid spatial compatibility effects. Finger movements were associated with number 1 for the index finger and number 2 for the middle finger. In the congruent conditions, the number associated with the moving finger appeared, while the incongruent condition consisted of nonmatched number and finger. Congruent and incongruent trials (rows 1 and 3 of panels *C* and *D*) were identical for both tasks and differed only for the instruction given: In the Finger Task (panel *C*), participants were explicitly asked to imitate the finger movements they saw while ignoring the numbers, while in the Number Task (panel *D*), they were asked to lift the finger associated with the shown number while ignoring the movements of the fingers. Neutral conditions (middle row of panels *C* and *D*) were different for the two tasks: In the Finger Task, only the moving hand was shown with no numbers presented; in the Number Task, the hand was displayed at rest while numbers, which are the relevant dimension in this task, appeared in the usual position.

Results

Evidence of Automatic Imitation before ccPAS.

We first evaluated behavioral performance before ccPAS. In the Number Task, we observed clear facilitatory and interference effects indicative of automatic imitation: Participants exhibited quicker RTs and higher accuracy in trials where the number (i.e., the task-relevant stimulus) was presented alongside a finger movement (i.e., the task-irrelevant stimulus) congruent with the number; conversely, they displayed slower and less accurate responses in trials featuring incongruent finger movements (*SI Appendix*, Fig. S1). Moreover, in the Finger Task, where participants were instructed to replicate observed finger movements, we observed interference effects from incongruent numbers, resulting in slower RTs and diminished accuracy (*SI Appendix*, Fig. S1). These effects were consistent across all groups prior to ccPAS administration.

No Effect of ccPAS on Voluntary Imitation or Arbitrary Visuomotor Mapping.

To examine the impact of ccPAS on performance, we integrated both RTs and Accuracy metrics into the Inverse Efficacy (IE) index by calculating the ratio between RTs and % accuracy for each trial type (37). This approach allowed us to assess ccPAS effects independently from speed/accuracy trade-off confounds. We first focused on

neutral trials, i.e., trials in which participants performed voluntary imitation (Finger Task) or followed arbitrary visuomotor mapping (Number Task) in the absence of task-irrelevant stimulus influence. The analysis revealed improved performance over time and across all groups, including ccPAS$_{Sham}$, likely reflecting practice effects (*SI Appendix*, Fig. S2) and suggesting no effect of ccPAS on goal-directed behavior across the two tasks.

PMv-to-M1 and SMA-to-M1 ccPAS Exert Opposite Influences on Interference Indices of Automatic Imitation.

To control for the unspecific practice-induced changes in IE, we computed facilitatory (congruent—neutral trials IE) and interference (incongruent—neutral trials IE) behavioral indices of automatic imitation. We first focused on automatic imitation by analyzing performance in the Number Task through a ccPAS group (ccPAS$_{PMv→M1}$, ccPAS$_{M1→PMv}$, ccPAS$_{SMA→M1}$; ccPAS$_{Sham}$) × Time (Pre, T0, T30) × Index (Facilitatory IE, Interference IE) ANOVA. The analysis showed the higher-order ccPAS × Time × Index interaction ($F = 3.92$, $P = 0.001$; $\eta_p^2 = 0.13$). Post hoc comparisons showed no between-group differences before ccPAS for either the facilitatory or the interference index (all $P \geq 0.06$). Moreover, while the facilitatory index remained stable over time (all $P \geq 0.19$; *SI Appendix*, Fig. S3), the interference index varied as a function of ccPAS and Time (Fig. 2*A*).

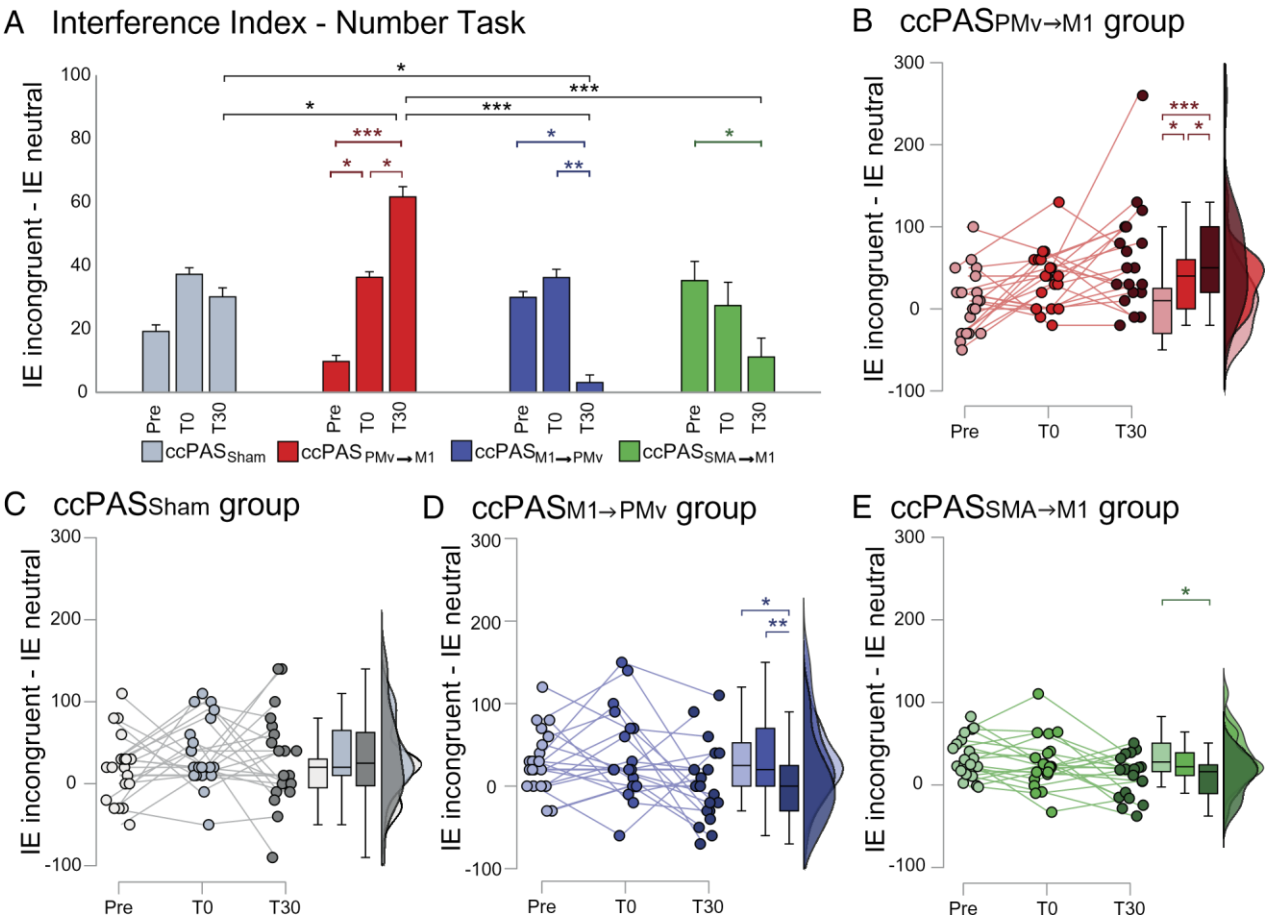

Fig. 2. (*A*) The interference index observed in incongruent trials of the Number Task, tapping into automatic imitation, changed as a function of time and ccPAS protocol. (*B–E*) Individual data across the four ccPAS groups. Following the ccPAS protocol, interference increased in the ccPAS$_{PMv→M1}$ group (*B*), remained unchanged in the ccPAS$_{Sham}$ group (*C*), and decreased in the ccPAS$_{SMA→M1}$ (*E*) and ccPAS$_{M1→PMv}$ (*D*) groups. Error bars represent one SEM. Asterisks indicate post-hoc comparisons (*$P \leq 0.05$; **$P \leq 0.01$; ***$P \leq 0.001$).

In the ccPAS$_{PMv→M1}$ group, the interference index increased from Pre to T0 ($P = 0.016$, *Cohen's d* = 0.56) and showed a more substantial increase at T30 (T30 vs. Pre: $P < 0.001$, *Cohen's d* = 0.59; T30 vs. T0: $P = 0.012$, *Cohen's d* = 0.36), reflecting enhanced automatic imitation. On the contrary, in the ccPAS$_{SMA→M1}$ group, the interference index decreased at T30 ($P = 0.032$, *Cohen's d* = 0.60) compared to Pre. In the ccPAS$_{M1→PMv}$ group, interference was

comparable at Pre and T0 ($P = 0.56$), but it declined at T30 relative to both Pre ($P = 0.012$, *Cohen's d* = 0.47) and T0 timepoints ($P = 0.002$, *Cohen's d* = 0.50). In the $ccPAS_{Sham}$ group, interference did not change between timepoints (all $P \geq 0.11$). Comparing the four ccPAS groups, at T30, the $ccPAS_{PMv\rightarrow M1}$ group showed greater interference when compared with all other groups (all $P \leq 0.011$, all *Cohen's d* ≥ 0.51), and the $ccPAS_{M1\rightarrow PMv}$ group showed reduced interference compared with the $ccPAS_{PMv\rightarrow M1}$ group ($P < 0.001$, *Cohen's d* = 1.03) and the $ccPAS_{Sham}$ group ($P = 0.036$, *Cohen's d* = 0.51), but not the $ccPAS_{SMA\rightarrow M1}$ group ($P = 0.52$). These patterns of changes in IE values were consistently mirrored by corresponding changes in RTs, with coherent trends also observed for accuracy (*SI Appendix*, Table S2).

To explore whether ccPAS drove similar effects on voluntary imitation, we also included the Finger Task in the analysis. The ccPAS group × Task × Time × Index ANOVA showed a significant quadruple interaction ($F_{6,152} = 3.77$, $P = 0.002$; $\eta_p^2 = 0.13$), suggesting a different impact of ccPAS on automatic (i.e., Number Task) as opposed to voluntary (i.e., Finger Task) imitation.

SMA-to-M1 ccPAS Attenuates Interference from Arbitrary S–R Associations during Voluntary Imitation.

A similar ccPAS × Time × Index ANOVA was conducted on Finger Task performance indices to study the effect of ccPAS on arbitrary S–R (number-to-finger) associations during voluntary imitation: The analysis revealed a significant main effect of Index ($F_{1,76} = 28.07$, $P < 0.001$; $\eta_p^2 = 0.27$), qualified by an Index × Time interaction ($F_{2,152} = 3.12$, $P = 0.047$; $\eta_p^2 = 0.04$, *SI Appendix*, Fig. S4), showing that while the facilitatory index remained stable across timepoints (all $P \geq 0.25$), the interference index decreased over time (Pre vs. T0: $P = 0.03$, *Cohen's d* = 0.20; Pre vs. T30: $P = 0.02$, *Cohen's d* = 0.22).

Although the main effect of, or interactions with the factor ccPAS did not reach significance (all $P \geq 0.17$), we performed planned comparisons to directly test whether reinforcing the SMA-to-M1 pathway would improve the ability to prevent interference in incongruent trials of the Finger Task too, which would support a general gating role of SMA. Four Bonferroni-corrected planned comparisons, one for each group, were computed comparing the interference index between Pre and T0-T30. We found that $ccPAS_{SMA\rightarrow M1}$ reduced the interference index ($P = 0.037$, Fig. 3*B*). In contrast, no impact of $ccPAS_{PMv\rightarrow M1}$, $ccPAS_{Sham}$, or $ccPAS_{M1\rightarrow PMv}$ was observed (all $P \geq 0.19$).

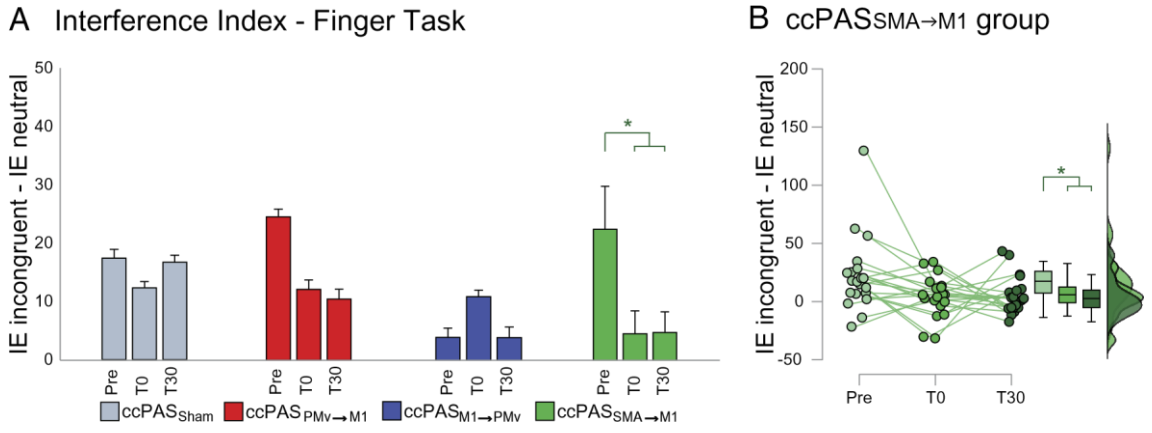

Fig. 3. (*A*) Interference index observed in incongruent trials of the Finger Task. (*B*) Individual data of the $ccPAS_{SMA\rightarrow M1}$ group. Following the ccPAS protocol, interference decreased only in the $ccPAS_{SMA\rightarrow M1}$ group. Asterisks indicate significant planned comparisons (*$P \leq 0.05$, Bonferroni corrected). Error bars represent 1 SEM.

ccPAS Drives Direction- Dependent Opposite Changes in Cortico-Spinal Motor Excitability.

While administering TMS pulses in the active ccPAS protocols, we induced motor- evoked potentials (MEPs) by suprathreshold stimulation of M1. This allowed us to monitor changes in motor excitability throughout the ccPAS procedure. The ccPAS ($ccPAS_{PMv\rightarrow M1}$, $ccPAS_{M1\rightarrow PMv}$ and $ccPAS_{SMA\rightarrow M1}$) × Epoch (1 to 6) ANOVA on MEP amplitudes (Fig. 4) recorded during the protocol (90 MEPs divided into 6 Epochs of 15 MEPs each) revealed a significant ccPAS × Epoch interaction ($F_{10,285} = 7.37$, $P < 0.001$, $\eta_p^2 = 0.21$): MEPs gradually increased during $ccPAS_{PMv\rightarrow M1}$ and $ccPAS_{SMA\rightarrow M1}$, while a reduction was observed during $ccPAS_{M1\rightarrow PMv}$ (see Fig. 4 for *P* values of all comparisons).

Relative to the first epoch, at Epoch 6 the $ccPAS_{PMv\rightarrow M1}$ group showed an average MEP increase of +0.39 mV (*Cohen's d* = 1.32), the $ccPAS_{SMA\rightarrow M1}$ group showed an increase of 0.30 mV (*Cohen's d* = 0.67), and the $ccPAS_{M1\rightarrow PMv}$ group a mean reduction of −0.33 mV (*Cohen's d* = 1.31).

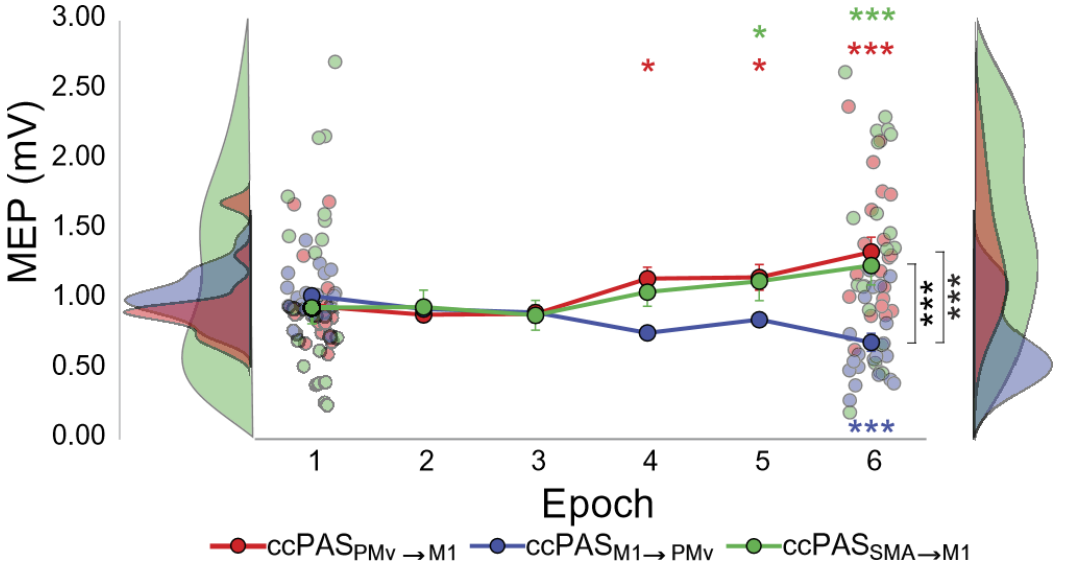

Fig. 4. Mean physiological changes induced by ccPAS during protocol administration (individual data shown at Epochs 1 and 6). In the $ccPAS_{PMv\rightarrow M1}$ and $ccPAS_{SMA\rightarrow M1}$ groups, there was a gradual increase in motor excitability, whereas in the $ccPAS_{M1\rightarrow PMv}$ group, there was a gradual decrease. Colored group asterisks indicate post hoc within-group differences relative to Epoch 1; black asterisks indicate post hoc differences between $ccPAS_{M1\rightarrow PMv}$ and other groups (*$P \leq 0.05$; **$P \leq 0.01$; ***$P \leq 0.001$). Error bars represent 1 SEM.

Discussion

The AON is a highly plastic system tuned to sensorimotor experience (38–41), and theoretical models have proposed Hebbian associative plasticity as a key mechanism for shaping the network's properties during development and learning (9, 42, 43). Prior noninvasive brain stimulation studies have suggested that frontal regions of the AON are relevant for automatic imitation, as targeting these regions attenuates/eliminates performance differences between congruent and incongruent trials in the imitation inhibition task (11, 23, 24, 42). However, none of these studies investigated the causal role of specific AON-to-M1 cortico-cortical pathways in automatic imitation, and causal evidence that the AON influences M1 to support automatic imitation remains elusive.

Using ccPAS to manipulate the strength of projections from the PMv and SMA to M1 through Hebbian STDP has advanced our understanding of the neural pathways that causally support and control automatic imitation and has clarified the distinct roles of PMv-to-M1 and SMA-to-M1 projections in modulating automatic motor imitation.

Enhancing connectivity from PMv to M1 ($ccPAS_{PMv\rightarrow M1}$) boosted automatic imitation while weakening it ($ccPAS_{M1\rightarrow PMv}$) led to its reduction. In contrast, reinforcing SMA-to-M1 projections ($ccPAS_{SMA\rightarrow M1}$) decreased automatic imitation. It should be noted that all active ccPAS protocols involved identical PMv, SMA, and M1 stimulations in terms of number of pulses and intensity and, hence, had similar impacts on the component elements of the respective circuits. Thus, behavioral effects cannot be attributed to modifications confined to PMv, SMA, or M1, but to the manipulation of the connectivity between them. Thus, our findings offer causal evidence of a double dissociation within AON-to-M1 projections, highlighting their plastic malleability and functional relevance to automatic imitation.

Automatic Imitation before ccPAS.

In the Pre session, participants displayed the hallmarks of automatic imitation: In incongruent trials of the Number Task—a modified version of Brass et al.' imitation inhibition task (5, 35)—the competition between short-term (weaker) number-to-movement associations established for the purpose of the task and long-term (stronger) finger-

to-movement automatic imitation associations led to strong interference effects, with longer RTs and lower accuracy, reflecting a consistent influence of the automatic imitative association between perceived and executed actions (2, 3, 5, 44). Conversely, observed actions in congruent trials facilitated performance, with shorter RTs and higher accuracy. It is assumed that automatic imitative S–R associations hold greater strength compared to the S–R number-to-movement associations established for the purpose of the Number Task (3). Indeed, we observed lower overall performance and more consistent facilitatory and interference effects of task-irrelevant stimuli in the Number Task compared to the Finger Task. Yet, a slight interference effect due to the competition between imitative responses and number-to-movement learned associations was also detected in incongruent trials of the Finger Task.

ccPAS over PMv- to- M1 Projections Selectively Modulates Automatic Imitation.

We found $ccPAS_{PMv\rightarrow M1}$ to enhance the interferential effect of automatic imitation; hence, our results speak against the hypothesis that the PMv and the inferior frontal cortex control imitative responses to comply with task rules and contextual information (23, 24). Instead, our findings support the hypothesis that PMv-to-M1 connections are spontaneously activated by observed actions (10, 22) and, through its copious projections to M1 (45, 46), facilitate the tendency to imitate them. Indeed, strengthening PMv-to-M1 connectivity through ccPAS did not lead to an improved ability to dampen the interferential effect induced by the observation of task-irrelevant actions, as would be expected under the assumption that the PMv-to-M1 pathway plays a control role. Interestingly, reversing the stimulation order of the PMv and M1 nodes ($ccPAS_{M1\rightarrow PMv}$) led to the opposite outcome and hindered automatic imitation, further supporting the causal role of the PMv- M1 pathway in this behavior. These bidirectional effects of ccPAS are consistent with previous studies, which found that the application of $ccPAS_{PMv\rightarrow M1}$, designed to induce long-term potentiation (LTP) via Hebbian STDP enhanced the strength of the PMv-to-M1 pathway, while $ccPAS_{M1\rightarrow PMv}$ weakened it (20, 25, 31, 32, 34, 36).

Our findings not only align with but also significantly expand upon existing evidence. For example, previous research on action observation has demonstrated that $ccPAS_{PMv\rightarrow M1}$ can enhance motor resonance in M1, as evidenced by increased MEP amplitudes in muscles involved in the observed actions (47). Notably, our study extends these physiological insights by clearly demonstrating a significant behavioral impact of $ccPAS_{PMv\rightarrow M1}$ on automatic imitation, thus bridging physiological processes with measurable behavioral effects. Furthermore, earlier noninvasive brain stimulation studies have explored the role of the human frontal cortex in imitation using both electrical and magnetic stimulation through online and offline approaches (11, 23, 24, 42). This body of work has suggested that the inferior frontal cortex, overlapping with the rostral PMv site targeted in our study, is critical for automatic imitation. In contrast, our study adopts a novel multisite methodology, showcasing the potential to enhance or impede automatic imitation by strengthening or weakening the connection between PMv and M1. Given our findings, which underscore the significance of PMv-M1 connectivity, one might speculate that prior studies focusing on the role of the inferior frontal cortex could have impacted the PMv-to-M1 pathway. This potential influence may have contributed to the effects on automatic imitation observed in these studies.

Critically, ccPAS-induced changes concerned only incongruent trials, i.e., trials entailing conflict between task rules and task-irrelevant stimuli. Indeed, although performance in conflict-free neutral trials improved over time in both tasks (*SI Appendix*, Fig. S2), likely due to practice, the ccPAS protocols had no differential impact. This is consistent with other studies showing no impact of premotor-to-M1 ccPAS on goal-oriented performance on simple visuomotor tasks (26, 31, 48).

These findings support the specificity of PMv-to-M1 projections in affecting long-term finger-to-action associations underlying automatic imitation—supporting the domain specificity of PMv-M1 connectivity (49, 50). In contrast, $ccPAS_{PMv\rightarrow M1}$ did not modulate the ability to carry out arbitrary number-to-movement associations established for the task, suggesting a separate route might be involved (51).

SMA-to -M1 Projections Are Critical for Goal-Directed Behavior in Conflict Conditions.

Manipulating the SMA- M1 pathway with ccPAS noticeably reduced automatic imitation, as indexed by improved performance on incongruent Number Task trials. Although the activation of the SMA during both action observation and execution is frequently reported (8, 20), its specific role within the AON remains poorly understood. SMA motor neurons exhibit state-dependent activation patterns based on contexts and task demands (17–19). Enhanced SMA activity during incongruent trials of the imitation inhibition task (21) has led scholars to propose that such activation during action observation serves a gating function, inhibiting motor output to prevent inadequate imitative responses

(16, 20). Our results provide causal evidence supporting this notion, showing that strengthening SMA-to-M1 connectivity improves control over interference in incongruent trials of the Number Task and increases cortico-spinal excitability.

More broadly, SMA is part of the multiple-demand network, activated under cognitively demanding and conflicting conditions to sustain performance (14, 17). This led us to hypothesize that strengthening connectivity between the SMA and M1 should, in principle, improve performance in incongruent trials of the Finger Task, too: Although less pronounced than in the Number Task, these trials also entail some level of conflict between the arbitrary number- to-action S–R associations (learned for the Number Task) and the imitative response to be produced. Our results confirmed this hypothesis, indicating that following $ccPAS_{SMA\rightarrow M1}$ participants improved their ability to suppress interference from task-irrelevant stimuli, supporting a broader cognitive control role of the SMA-to-M1 pathway.

ccPAS Affects Only the Interferential Component of Automatic Imitation.

Prior brain stimulation studies on automatic imitation have commonly quantified the phenomenon as the performance difference between congruent and incongruent trials of the imitation inhibition task (15, 23, 24, 42), which makes it impossible to qualify whether brain stimulation has acted on the facilitatory or interference components of automatic imitation, or both. This is a relevant issue as the two effects may involve partially distinct neural mechanisms (11–15). To address this outstanding issue, we included a neutral condition in the imitation inhibition task to quantify both facilitatory and interference effects. As we anticipated, we observed modulations only in the interferential component of automatic imitation. While we do not rule out the possibility that facilitatory effects could also be mediated by AON projections to M1, the convergence of goal-oriented (i.e., task- based) and automatic components of behavior may render these responses less amenable to TMS- induced plastic changes— particularly in the current study where general performance increase (*SI Appendix*, Fig. S2) could lead to ceiling effects.

Conversely, interference occurs in conditions of competition (2, 3): In incongruent trials, rule-based responses based on short-term (weaker) number-to-movement associations established for the purpose of the task compete with long-term (stronger) finger-to-movement associations. Our study provides causal evidence that in such conflicting conditions, driving associative plasticity between key nodes of the AON and the ipsilateral M1 can bias the competition between rule-based or automatic behavior, with distinct effects based on the manipulated pathway, so that enhancing PMv-to-M1 connectivity via $ccPAS_{PMv\rightarrow M1}$ reinforces automatic behavior, while enhancing SMA-to-M1 connectivity via $ccPAS_{SMA\rightarrow M1}$ improves control over it. Thus, these findings offer causal evidence of the neural mechanisms that underlie and control automatic imitation in conflict conditions mediated by cortico-cortical AON-to-M1 projections.

Temporal Dynamics of Physiological and Behavioral Changes Following ccPAS.

Taking advantage of recent evidence on the bidirectional manipulation of associative plasticity in the PMv-to-M1 pathway (25, 26, 28, 30–32, 34, 47), the present study compared the aftereffects of $ccPAS_{PMv\rightarrow M1}$ and $ccPAS_{M1\rightarrow PMv}$. These protocols displayed symmetrical opposite effects, with the former increasing and the latter decreasing automatic imitation. This diverging effect was anticipated by neurophysiological indices of connectivity manipulation observed during the protocol: $ccPAS_{PMv\rightarrow M1}$ induced a gradual increase and $ccPAS_{M1\rightarrow PMv}$ induced a gradual decrease in MEP amplitude during the protocol's administration, indexing rapid growing of facilitation/inhibition of motor excitability as a function of the repeated activation of the PMv-M1 circuit in the two opposite directions (34, 36). During $ccPAS_{PMv\rightarrow M1}$, in each TMS pair, the cortico-cortical volley elicited by PMv stimulation (first pulse) would reach M1 slightly before the exogenous M1 stimulation (second pulse), resulting in a convergent activation of M1 optimal for the establishment of STDP (52, 53), reflected in an LTP-like effect (Fig. 4). On the contrary, reversing the pattern and stimulating M1 before PMv ($ccPAS_{M1\rightarrow PMv}$) would exogenously reproduce patterns of synaptic activity where the post-synaptic area is activated before the presynaptic one, known to produce long-term depression (LTD) (54). This repeated paired stimulation would thus weaken the PMv input to M1, leading to reduced motor excitability (Fig. 4). It should be noted that these opposite influences of reversing the paired stimulation during ccPAS are specific to the PMv-to-M1 pathway (25, 36), whereas reversing the order of the pulses in ccPAS protocols applied to the SMA-to-M1 pathway do not result in opposite modulation of motor excitability due to an asymmetry in the SMA-to-M1 and M1-to-SMA cortico-cortical interactions (34). Therefore, it remains to be determined whether ccPAS protocols adept at weakening SMA-to-M1 projections have an impact on automatic imitation. Nonetheless, the emergence of physiological and behavioral expression of plasticity during and following stimulation is consistent

with prior ccPAS studies (25, 26, 29, 47) and, in general, with the time course of Hebbian plasticity (51) and LTP/LTD-like effects in the human motor system (55, 56).

Materials and Methods

Participants. Eighty healthy, naive right-handed participants (31 males, mean age 22.5 ± 2.2 y, age range: 19 to 30) with normal or corrected-to-normal visual acuity took part in the study. All participants gave written informed consent, and none reported contraindications or adverse reactions to TMS (57). The experimental procedures were in accordance with the 1964 Declaration of Helsinki (58) and approved by the Bioethical Committee of the University of Bologna.

The sample size was determined using G*Power 3.1.9.4 for a mixed-design ANOVA with within-between factors, covering 4 groups and 6 measurements (3 blocks × 2 tasks). We aimed to achieve a statistical power ($1-\beta$) of 0.95 and set the significance level (α) at 0.05. Although current ccPAS research typically reports moderate-to-large effect sizes, we conservatively anticipated a small-to-moderate effect size (f) of 0.18 in our study. The power analysis indicated that at least 76 participants were necessary to adequately power the study. To mitigate the risk of data loss due to technical issues or other unforeseen circumstances, we enrolled 80 participants. All participants were tested in a single ccPAS group. Three participants initially assigned to the $ccPAS_{SMA\rightarrow M1}$ protocol were excluded during a preliminary phase because proper placement of the two coils was unfeasible due to head size constraints, preventing ccPAS administration. These participants were replaced, ensuring that a total of 80 participants successfully completed the experiment, with 20 participants maintained in each group.

General Experimental Design and Procedures. To test whether the exogenous manipulation of PMv- to- M1 or SMA- to- M1 connectivity affects automatic imitation, we repeatedly targeted PMv/SMA and M1 using ccPAS (25, 26, 28, 30, 34). We measured the peak-to-peak amplitude of MEPs induced by TMS pulses during the ccPAS protocol to assess its neurophysiological correlates (34, 36). To test the behavioral effects of ccPAS, we asked participants to perform a voluntary imitation task (i.e., the Finger Task) and an imitation inhibition task (i.e., the Number Task), specifically assessing automatic imitation (5). Participants familiarized with the behavioral tasks for ~2 min (training phase), and then, their performance was recorded in three experimental timepoints, i.e., before the ccPAS (Pre), immediately after (T0), and at 30 min after the end of the ccPAS (T30). Each timepoint lasted about ~10 min (Fig. 1*A*). The entire experiment lasted approximately 2.5 h. Participants were randomly assigned to one of four groups, according to the administered ccPAS protocol they underwent (see *SI Appendix*, Table S1 for demographic details). A preliminary version of the present study was reported in the Ph.D. thesis of the first author (59).

Behavioral Tasks. Two tasks were performed at each timepoint, in counterbalanced order between subjects: the Finger Task (voluntary imitation task) and the Number Task (automatic imitation task) (5). Participants were seated ~80 cm from the screen, and the images on the monitor covered a visual angle of ~10° vertically and ~6.5° horizontally. Both tasks included congruent, neutral, and incongruent trials (Fig. 1*C* and *D*). Pictures depicting resting/moving hands and symbolic cues (numbers "1" or "2") were presented in various combinations. The crucial difference between the Finger and the Number Task consisted of the experimental instructions, reflecting the relevant dimension of the task. In the Finger Task (Fig. 1*C*), participants were asked to imitate the finger movements displayed on the screen irrespective of the number shown; in the Number Task (Fig. 1*D*), participants were given a number- to-finger association (lift the index finger when presented with number "1," lift the middle finger when presented with number "2") and asked to follow it ignoring the observed movement. In both tasks, trials were classified as congruent when the number and the lifting finger matched (e.g., "1" and lifting of the index finger were displayed) or incongruent when they did not match (e.g., "1" and lifting of the middle finger). Neutral trials served as a control/baseline condition depicting only the task- relevant dimension: In the Finger Task, neutral trials showed only the finger movement (Fig. 1*C*); in the Number Task, neutral trials showed only the number (Fig. 1*D*).

Each trial started with a picture showing a resting hand (500 ms), followed by the trial-relevant screen (68 ms). Then, the same initial resting hand was shown again (560 ms) (5), and finally, an intertrial fixation cross was displayed for a random interval (2 to 3 s). During the tasks, participants were asked to continuously press two keys labeled "1" and "2" with their right index and middle fingers, respectively. They were instructed to lift the appropriate finger, releasing the key, as soon as they saw the task-relevant dimension in the second picture and subsequently replace the finger on the same key.

The training phase consisted of 24 trials. Each testing block consisted of 120 trials per task (40 congruent, 40 neutral, and 40 incongruent). To avoid the confound of spatial compatibility (60), hand stimuli were rotated 90° counterclockwise to obtain a pure assessment of automatic imitation (3, 35, 47, 61, 62).

ccPAS Protocol. The ccPAS was delivered using two 50-mm figure-of-eight iron-branding coils, each connected to a Magstim 200_2 monophasic stimulator (The Magstim Company). In the $ccPAS_{PMv\rightarrow M1}$, $ccPAS_{M1\rightarrow PMv}$ and $ccPAS_{Sham}$ groups, one coil was placed over the left PMv and the other over the left M1; in the $ccPAS_{SMA\rightarrow M1}$ group, one coil was placed over the left SMA and the other over the left M1. Ninety pairs of TMS pulses were delivered continuously at a rate of 0.1 Hz for ~15 min (25, 26, 30, 34, 47). In each pair, the interstimulus interval (ISI) between PMv, SMA, and M1 was 8 ms. This ISI was selected according to prior dual-coil TMS evidence that PMv or SMA conditioning influences MEPs induced by a test pulse over M1 administered after 8 ms (63–65). Thus, on each pair of the $ccPAS_{PMv\rightarrow M1}$ and $ccPAS_{SMA\rightarrow M1}$ protocols, the corticocortical volley elicited by PMv/ SMA stimulation reached M1 immediately before its direct stimulation, resulting in convergent activation of pre- and postsynaptic neurons, instrumental to the establishment of STDP (25, 28, 31). Of note, this specific ISI has been employed to successfully modulate the PMv-M1 and SMA-M1 circuits using ccPAS (30, 34, 47).

The $ccPAS_{PMv\rightarrow M1}$ group received a protocol with the pulse over PMv always delivered before the one administered over M1; the $ccPAS_{M1\rightarrow PMv}$ group received a protocol with the pulse pairs in the reversed order; the $ccPAS_{SMA\rightarrow M1}$ group received a ccPAS protocol with the pulse over SMA always delivered before the one administered over M1; the $ccPAS_{Sham}$ group received sham stimulations. A custom- made MATLAB script (MathWorks) controlled both stimulators triggering the pulses. In the $ccPAS_{PMv\rightarrow M1}$, $ccPAS_{M1\rightarrow PMv}$, and $ccPAS_{Sham}$ groups, the coil stimulating PMv was placed tangentially to the scalp and oriented to induce an anterior-to-posterior and lateral-to-medial current flow in the brain (30, 31, 47); in the $ccPAS_{SMA\rightarrow M1}$ the coil stimulating SMA was oriented to induce an anterior-to-posterior current in the brain (66). In all groups, the coil over M1 was held tangentially to the scalp, at ~45° angle to the midline, inducing a posterior-to-anterior current flow in the brain.

During the ccPAS protocol, participants kept their eyes open and hand muscles relaxed; thus, the ccPAS was administered in a resting-state condition. To assess changes in motor excitability, MEPs induced by stimulation of the left M1 were recorded from the right first dorsal interosseous (FDI) muscle using disposable Ag/ AgCl surface electrodes placed in a belly-tendon montage, with the ground electrode placed on the right wrist. EMG signals were acquired using a Biopac MP-35 (Biopac) electromyograph, band-pass filtered (30 to 500 Hz), digitized at a sampling rate of 10 kHz, and stored for offline analysis. Peak-to-peak MEP amplitudes were measured in mV. MEPs were grouped into 6 epochs of 15 MEPs each (Epoch 1: MEP 1 to 15; Epoch 2: MEP 16 to 30; Epoch 3: MEP 31 to 45; Epoch 4: MEP 46 to 60; Epoch 5: MEP 61 to 75; and Epoch 6: MEP 76 to 90), averaged, and analyzed.

In the active ccPAS groups ($ccPAS_{PMv\rightarrow M1}$, $ccPAS_{M1\rightarrow PMv}$, and $ccPAS_{SMA\rightarrow M1}$), the conditioning intensity (PMv or SMA) corresponded to 90% of the individual's resting motor threshold (rMT), defined as the minimum stimulator output intensity that induced a MEP with a peak-to-peak amplitude $\geq$ 50 μV in 5 out of 10 consecutive trials. M1 stimulation was adjusted to evoke MEPs of about 1 mV amplitude (26, 30, 36, 47). We implemented a double-blind procedure: Participants were blinded to group allocation, and the experimenters who collected behavioral data were also unaware of the ccPAS conditions. The experimenters who administered the ccPAS were not blinded to group allocation, as they needed to set the TMS parameters (i.e., order of pulses, ISI, and orientation of the coils).

Neuronavigation. The left M1 site was identified functionally as the FDI motor hotspot, whereas the left PMv and SMA were identified using the SofTaxic Navigator System (Electro Medical System). A uniform representation of the scalp was reconstructed by recording the position of four skull landmarks (nasion, inion, and the two preauricular points) and ~80 points over the scalp using a Polaris Vicra infrared camera (Northern Digital) and an individual estimated MRI was constructed through a 3D warping procedure fitting a high-resolution template to the participants' scalp model and craniometric points. To target the PMv, the coil was placed at the border between the anterior sector of the ventral premotor cortex and the posterior sector of the inferior frontal gyrus, corresponding to the following Talairach coordinates: x = −54, y = 10, z = 24, previously used to modulate AON functioning (49, 67), and closely corresponding to brain imaging meta-analysis of action imitation (8, 68) and brain stimulation studies testing automatic imitation (11, 42). The SMA was stimulated approximately 4 cm anterior to the vertex on the sagittal midline (69), corresponding to the following Talairach coordinates: x = −2, y = −7, z = 55 (70). Using the Softaxic Neuronavigator, we automatically estimated the Talairach coordinates corresponding to the projections of the left PMv, SMA, and M1 on the brain surface of the MRI-constructed stereotaxic template (Fig. 1*B*).

Statistical Analysis. ANOVAs and nonparametric tests ($\chi 2$) were performed to compare the four groups by gender and motor excitability (*SI Appendix*, Table S1). Mean reaction times (RTs) and accuracy (% of correct responses; %Corr) were recorded for each session. Trials with RTs below 80 ms or above 800 ms, as well as trials with both keys released and anticipations, were classified as errors and excluded from the analysis (5) (2.9% of the total). In a preliminary analysis, we assessed task performance before any ccPAS manipulation: RTs were assessed in the

Presession using a mixed-factors ANOVA with ccPAS ($ccPAS_{Sham}$, $ccPAS_{PMv\rightarrow M1}$, $ccPAS_{M1\rightarrow PMv}$, $ccPAS_{SMA\rightarrow M1}$) as the between-subjects factor and Task (Finger, Number) and Trial (Congruent, Neutral, Incongruent) as the within-subjects factors. Due to the extreme skewness of %Corr data (Lilliefors $P < 0.001$), nonparametric analyses were conducted using Friedman ANOVAs, Kruskal–Wallis ANOVAs, and Wilcoxon paired tests to compare accuracy between trial types and groups.

To assess the impact of ccPAS manipulation on behavioral outcomes, we integrated measures of performance speed and accuracy through the computation of a unified metric known as the Inverse Efficacy (IE) index, calculated as the ratio between RTs and the proportion of correct responses for each trial type in both tasks (37, 71). This was employed to ensure that changes in behavior were not driven by a strategic adjustment of criteria or a mere prioritization of speed over accuracy, and vice versa, thus providing a robust metric to discern genuine effects of ccPAS manipulation on performance.

We first tested whether ccPAS impacted voluntary imitation by analyzing neutral trials of the Finger Task using a mixed- factors ccPAS ($ccPAS_{Sham}$, $ccPAS_{PMv\rightarrow M1}$, $ccPAS_{M1\rightarrow PMv}$, $ccPAS_{SMA\rightarrow M1}$) x Time (Pre, T0, T30) ANOVA. Then, this analysis was extended to neutral trials of the Number Task to test the effect of ccPAS on goal-oriented behavior (*SI Appendix*, Fig. S2). In the main analysis, neutral trials were used as a baseline to compute indices of facilitation for congruent trials (IE congruent–IE neutral) and interference for incongruent trials (IE incongruent–IE neutral) (5). These indices were analyzed using a mixed-factors ANOVA with ccPAS group as a between-subjects factor and Task (Finger, Number), Time, and Index (Facilitatory, Inhibitory) as within-subject factors.

Peak-to-peak MEP amplitudes induced by active ccPAS protocols were automatically extracted using a custom-made MATLAB script, grouped into 6 epochs of 15 MEPs each, and averaged. Because background EMG affects motor excitability, MEPs preceded by background EMG activity that deviated by more than 2 SD from the individual mean were excluded from the analysis (≤3.1%). Mean MEP amplitudes were analyzed using a two-way ANOVA with ccPAS ($ccPAS_{PMv\rightarrow M1}$, $ccPAS_{M1\rightarrow PMv}$, and $ccPAS_{SMA\rightarrow M1}$) as the between-subjects factor and Epoch (1 to 6) as the within-subjects factor.

In all the ANOVAs, when appropriate, post hoc analyses were conducted using Duncan's post hoc test to correct for multiple comparisons, whereas in nonparametric analyses, *P*-levels were adjusted using the Bonferroni correction. Partial eta squared (η_p^2) was computed as a measure of effect size for significant main effects and interactions in the ANOVA; *Cohen's d* indices were computed as a measure of effect size for post hoc comparisons. For nonparametric Wilcoxon comparisons on %Corr, effect sizes were estimated by approximating *z*-scores to *r*-values. All analyses were conducted using STATISTICA v. 12.

Data, Materials, and Software Availability. All data have been deposited in OSF (https://osf.io/htwjv) (72). All other data are included in the manuscript and/or *SI Appendix*.

ACKNOWLEDGMENTS. This work was supported by a Bial Foundation grant (304/2022) awarded to A.A. This work was also supported by #NEXTGENERATIONEU (NGEU) and funded by the Ministry of University and Research (MUR), National Recovery and Resilience Plan (NRRP), project MNESYS (PE0000006). A Multiscale integrated approach to the study of the nervous system in health and disease (DN. 1553 October 11, 2022); FISM—Fondazione Italiana Sclerosi Multipla (2022/R-Single/071) and financed or cofinanced with the "5‰" public funding; Fondazione del Monte di Bologna e Ravenna (1402bis/2021); Universidad Católica Del Maule (CDPDS2022) awarded to A.A.; and a grant from the Chilean National Agency for Research and Development (Fondequip EQM210128) awarded to B.L.

Author contributions: A.A. designed research; S.T., F.F., and N.B. performed research; S.T., F.F., and B.L. contributed new reagents/analytic tools; S.T., F.F., N.B., C.S., and A.A. analyzed data; F.F., N.B., C.S., and B.L. reviewed the manuscript; and S.T., M.C., and A.A. wrote the paper.

References

1. T. L. Chartrand, J. A. Bargh, The Chameleon effect: The perception- behavior link and social interaction. *J. Person. Soc. Psychol.* **76**, 893e910 (1999).
2. C. Heyes, Automatic imitation. *Psychol. Bull.* **137**, 463–483 (2011).
3. E. Cracco *et al.*, Automatic imitation: A meta- analysis. *Psychol. Bull.* **144**, 453–500 (2018).

4. L. M. Sacheli, S. M. Aglioti, M. Candidi, Social cues to joint actions: The role of shared goals. *Front Psychol.* **6**, 1034 (2015).
5. M. Brass, H. Bekkering, W. Prinz, Movement observation affects movement execution in a simple response task. *Acta Psychol.* **106**, 3–22 (2001).
6. G. Barchiesi, L. Cattaneo, Early and late motor responses to action observation. *Soc. Cognit. Affect. Neurosci.* **8**, 711–719 (2013).
7. M. Brass, C. Heyes, Imitation: Is cognitive neuroscience solving the correspondence problem? *Trends Cognit. Sci.* **9**, 489–495 (2005).
8. S. Caspers, K. Zilles, A. R. Laird, S. B. Eickhoff, ALE meta- analysis of action observation and imitation in the human brain. *Neuroimage* **50**, 1148–1167 (2010).
9. R. Cook, G. Bird, C. Catmur, C. Press, C. Heyes, Mirror neurons: From origin to function. *Behav. Brain Sci.* **37**, 177–192 (2014).
10. G. Rizzolatti, L. Cattaneo, M. Fabbri-Destro, S. Rozzi, Cortical mechanisms underlying the organization of goal-directed actions and mirror neuron -based action understanding. *Physiol. Rev.* **94**, 655–706 (2014).
11. N. Bien, A. Roebroeck, R. Goebel, A. T. Sack, The brain's intention to imitate: The neurobiology of intentional versus automatic imitation. *Cerebral Cortex.* **19**, 2338–2351 (2009).
12. M. Brass, P. Ruby, S. Spengler, Inhibition of imitative behaviour and social cognition. *Philos. Trans. R. Soc. B: Biol. Sci.* **364**, 2359–2367 (2009).
13. K. A. Cross, S. Torrisi, E. A. R. Losin, M. Iacoboni, Controlling automatic imitative tendencies: Interactions between mirror neuron and cognitive control systems. *Neuroimage* **83**, 493–504 (2013).
14. K. M. Darda, R. Ramsey, The inhibition of automatic imitation: A meta- analysis and synthesis of fMRI studies. *NeuroImage* **197**, 320–329 (2019).
15. S. Sowden, C. Catmur, The role of the right temporoparietal junction in the control of imitation. *Cerebral Cortex.* **25**, 1107–1113 (2015).
16. V. Gazzola, C. Keysers, The observation and execution of actions share motor and somatosensory voxels in all tested subjects: Single- subject analyses of unsmoothed fMRI data. *Cerebral Cortex* **19**, 1239–1255 (2009).
17. P. Nachev, C. Kennard, M. Husain, Functional role of the supplementary and pre-supplementary motor areas. *Nat. Rev. Neurosci.* **9**, 856–869 (2008).
18. F. Bonini *et al.*, Action monitoring and medial frontal cortex: Leading role of supplementary motor area. *Science* **343**, 888–891 (2014).
19. G. Rizzolatti *et al.*, Neurons related to reaching- grasping arm movements in the rostral part of area 6 (area 6aβ). *Exp. Brain Res.* **82**, 337–350 (1990).
20. R. Mukamel, A. D. Ekstrom, J. Kaplan, M. Iacoboni, I. Fried, Single- neuron responses in humans during execution and observation of actions. *Curr. Biol.* **20**, 750–756 (2010).
21. K. M. Darda, E. E. Butler, R. Ramsey, Functional specificity and sex differences in the neural circuits supporting the inhibition of automatic imitation. *J. Cognit. Neurosci.* **30**, 914–933 (2018).
22. M. Iacoboni *et al.*, Cortical mechanisms of human imitation. *Science* **286**, 2526–2528 (1999).
23. J. Hogeveen *et al.*, Task- dependent and distinct roles of the temporoparietal junction and inferior frontal cortex in the control of imitation. *Soc. Cognit. Affect. Neurosci.* **10**, 1003–1009 (2015).
24. S. Nobusako *et al.*, Transcranial direct current stimulation of the temporoparietal junction and inferior frontal cortex improves imitation- inhibition and perspective- taking with no effect on the autism- spectrum quotient score. *Front Behav. Neurosci.* **11**, 84 (2017).
25. E. R. Buch, V. M. Johnen, N. Nelissen, J. O'Shea, M. F. S. Rushworth, Noninvasive associative plasticity induction in a corticocortical pathway of the human brain. *J. Neurosci.* **31**, 17669–17679 (2011).
26. F. Fiori, E. Chiappini, A. Avenanti, Enhanced action performance following TMS manipulation of associative plasticity in ventral premotor-motor pathway. *NeuroImage* **183**, 847–858 (2018).
27. J. C. Hernandez- Pavon, A. San Agustín, M. C. Wang, D. Veniero, J. L. Pons, Can we manipulate brain connectivity? A systematic review of cortico- cortical paired associative stimulation effects. *Clin. Neurophysiol.* **154**, 169–193 (2023).
28. V. M. Johnen *et al.*, Causal manipulation of functional connectivity in a specific neural pathway during behaviour and at rest. *eLife* **2015**, e04585 (2015).
29. V. Romei, E. Chiappini, P. B. Hibbard, A. Avenanti, Empowering Reentrant Projections from V5 to V1 Boosts Sensitivity to Motion. *Curr. Biol.* **26**, 2155–2160 (2016).

30. S. Turrini *et al.*, Cortico-cortical paired associative stimulation (ccPAS) over premotor -motor areas affects local circuitries in the human motor cortex via Hebbian plasticity. *NeuroImage* **271**, 120027 (2023).
31. A. Sel *et al.*, Increasing and decreasing interregional brain coupling increases and decreases oscillatory activity in the human brain. *Proc. Natl. Acad. Sci. U.S.A.* **118**, 1–9 (2021).
32. J. Trajkovic, V. Romei, M. F. S. Rushworth, A. Sel, Changing connectivity between premotor and motor cortex changes inter-areal communication in the human brain. *Progr. Neurobiol.* **228**, 102487 (2023).
33. N. Arai *et al.*, State- dependent and timing-dependent bidirectional associative plasticity in the human SMA- M1. *Network* **31**, 15376–15383 (2011).
34. N. Bevacqua *et al.*, Cortico- cortical paired associative stimulation highlights asymmetrical communication between rostral premotor cortices and primary motor cortex. *Brain Stimul. Basic, Transl. Clin. Res. Neuromodul.* **17**, 89–91 (2024).
35. J. Cook, G. Bird, Social attitudes differentially modulate imitation in adolescents and adults. *Exp. Brain Res.* **211**, 601–612 (2011).
36. S. Turrini *et al.*, Gradual enhancement of corticomotor excitability during cortico-cortical paired associative stimulation. *Sci. Rep.* **12**, 14670 (2022).
37. J. T. Townsend, F. G. Ashby, *The Stochastic Modeling of Elementary Psychological Processes (Part 1)* (Cambridge University Press, 1983).
38. B. Calvo- Merino, D. E. Glaser, J. Grèzes, R. E. Passingham, P. Haggard, Action observation and acquired motor skills: An FMRI study with expert dancers. *Cerebral Cortex* **15**, 1243–1249 (2005).
39. C. Catmur, V. Walsh, C. Heyes, Sensorimotor learning configures the human mirror system. *Curr. Biol.* **17**, 1527–1531 (2007).
40. E. S. Cross, A. F. D. C. Hamilton, S. T. Grafton, Building a motor simulation de novo: Observation of dance by dancers. *Neuroimage* **31**, 1257–1267 (2006).
41. G. Guidali, M. I. S. Carneiro, N. Bolognini, Paired associative stimulation drives the emergence of motor resonance. *Brain Stimul.* **13**, 627–636 (2020).
42. C. Catmur, V. Walsh, C. Heyes, Associative sequence learning: The role of experience in the development of imitation and the mirror system. *Philos. Trans. R. Soc. B: Biol. Sci.* **364**, 2369–2380 (2009).
43. C. Keysers, V. Gazzola, Hebbian learning and predictive mirror neurons for actions, sensations and emotions. *Philos. Trans. R. Soc. B: Biol. Sci.* **369**, 20130175–20130175 (2014).
44. C. Catmur, Automatic imitation? Imitative compatibility affects responses at high perceptual load. *J. Exp. Psychol. Hum. Percep. Performance* **42**, 530 (2016).
45. H. Shimazu, M. A. Maier, G. Cerri, P. A. Kirkwood, R. N. Lemon, Macaque ventral premotor cortex exerts powerful facilitation of motor cortex outputs to upper limb motoneurons. *J. Neurosci.* **24**, 1200–1211 (2004).
46. H. Tokuno, A. Nambu, Organization of nonprimary motor cortical inputs on pyramidal and nonpyramidal tract neurons of primary motor cortex: An electrophysiological study in the macaque monkey. *Cerebral Cortex Cortex* **10**, 58–68 (2000).
47. E. Chiappini *et al.*, Driving Hebbian plasticity over ventral premotor-motor projections transiently enhances motor resonance. *Brain Stimul.* **17**, 211–220 (2024).
48. S. Turrini *et al.*, Transcranial cortico- cortical paired associative stimulation (ccPAS) over ventral premotor- motor pathways enhances action performance and corticomotor excitability in young adults more than in elderly adults. *Front Aging Neurosci.* **15**, 1119508 (2023).
49. A. Avenanti, R. Paracampo, L. Annella, E. Tidoni, S. M. Aglioti, Boosting and decreasing action prediction abilities through excitatory and inhibitory tDCS of inferior frontal cortex. *Cerebral Cortex* **28**, 1282–1296 (2018).
50. R. P. Spunt, R. Adolphs, A new look at domain specificity: Insights from social neuroscience. *Nat. Rev. Neurosci.* **18**, 559–567 (2017).
51. J. O'Shea, C. Sebastian, E. D. Boorman, H. Johansen- Berg, M. F. S. Rushworth, Functional specificity of human premotor- motor cortical interactions during action selection. *Eur. J. Neurosci.* **26**, 2085–2095 (2007).
52. N. Caporale, Y. Dan, Spike timing- dependent plasticity: A Hebbian learning rule. *Annu. Rev. Neurosci.* **31**, 25–46 (2008).
53. D. Hebb, *The Organisation of Behaviour* (NY: John Wiley and Sons, New York, 1949).
54. J. C. Magee, D. Johnston, A synaptically controlled, associative signal for Hebbian plasticity in hippocampal neurons. *Science* **275**, 209–213 (1997).

55. Y. Z. Huang, M. J. Edwards, E. Rounis, K. P. Bhatia, J. C. Rothwell, Theta burst stimulation of the human motor cortex. *Neuron* **45**, 201–206 (2005).
56. K. Stefan, E. Kunesch, L. G. Cohen, R. Benecke, J. Classen, Induction of plasticity in the human motor cortex by paired associative stimulation. *Brain* **123**, 572–584 (2000).
57. S. Rossi *et al.*, Safety and recommendations for TMS use in healthy subjects and patient populations, with updates on training, ethical and regulatory issues: Expert Guidelines. *Clin. Neurophysiol.* **132**, 269–306 (2021).
58. WMA, World Medical Association Declaration of Helsinki: Ethical principles for medical research involving human subjects. *Jama* **310**, 2191–2194 (2013).
59. S. Turrini, "Induction of Hebbian associative plasticity through paired non-invasive brain stimulation of premotor- motor areas to elucidate the network's functional role", Dissertation thesis, Alma Mater Studiorum Università di Bologna. Dottorato di ricerca in Psychology, 35th cycle (2023), 10.48676/unibo/amsdottorato/10591.
60. K. Czekóová *et al.*, Imitation or polarity correspondence? Behavioural and neurophysiological evidence for the confounding influence of orthogonal spatial compatibility on measures of automatic imitation. *Cogn Affect Behav. Neurosci.* **21**, 212–230 (2021).
61. C. Catmur, C. Heyes, Time course analyses confirm independence of imitative and spatial compatibility. *J. Exp. Psychol.: Hum. Percept. Performance* **37**, 409 (2011).
62. R. P. Cooper, C. Catmur, C. Heyes, Are automatic imitation and spatial compatibility mediated by different processes? *Cognit. Sci.* **37**, 605–630 (2013).
63. M. Davare, R. Lemon, E. Olivier, Selective modulation of interactions between ventral premotor cortex and primary motor cortex during precision grasping in humans. *J. Physiol.* **586**, 2735–2742 (2008).
64. C. Neige *et al.*, Connecting the dots: Harnessing dual- site transcranial magnetic stimulation to quantify the causal influence of medial frontal areas on the motor cortex. *Cerebral Cortex* **33**, 11339–11353 (2023).
65. B. K. Rurak, J. P. Rodrigues, B. D. Power, P. D. Drummond, A. M. Vallence, Reduced SMA-M1 connectivity in older than younger adults measured using dual-site TMS. *Eur. J. Neurosci.* **54**, 6533–6552 (2021).
66. F. Fiori *et al.*, Long- latency modulation of motor cortex excitability by ipsilateral posterior inferior frontal gyrus and pre- supplementary motor area. *Sci. Rep.* **6**, 1–11 (2016).
67. A. Avenanti, L. Annella, M. Candidi, C. Urgesi, S. M. Aglioti, Compensatory plasticity in the action observation network: Virtual lesions of STS enhance anticipatory simulation of seen actions. *Cerebral Cortex* **23**, 570–580 (2013).
68. G. Papitto, A. D. Friederici, E. Zaccarella, The topographical organization of motor processing: An ALE meta-analysis on six action domains and the relevance of Broca's region. *NeuroImage* **206**, 116321 (2020).
69. R. B. Mars *et al.*, Short- latency influence of medial frontal cortex on primary motor cortex during action selection under conflict. *J. Neurosci.* **29**, 6926–6931 (2009).
70. M. A. Mayka, D. M. Corcos, S. E. Leurgans, VDE., Three- dimensional locations and boundaries of motor and premotor cortices as defined by functional brain imaging: A metaanalysis. *NeuroImage* **31**, 1453–1474 (2006).
71. P. O. Jacquet, A. Avenanti, Perturbing the action observation network during perception and categorization of actions' goals and grips: State- dependency and virtual lesion TMS effects. *Cerebral Cortex* **25**, 598–608 (2015).
72. S. Turrini, A. Avenanti, Spike- timing- dependent plasticity induction reveals dissociable supplementary– and premotor–motor pathways to automatic imitation. OSF. https://osf.io/htwjv. Deposited 25 April 2024.